Indian Journal of Chemistry
Vol. 64, October 2025, pp. 942-952
DOI: 10.56042/ijc.v64i10.20809

Synthesis of bioactive aryl anilides using solid acidic $FeCl_3$-Bentonite catalyst: DFT analysis, molecular docking and ADMET property evaluation

I Muthuvel[†a,b], J Divya[a], P Gayathri[a], S Balasundari[a], P Sudha[a], C Palanivel[c], B Krishnakumar[†d,e], V Manikandan[f], Abdullah K Alanazi[g] & G Thirunarayanan*[a]

[a] Department of Chemistry, Annamalai University, Annamalainagar 608 002, Tamil Nadu, India

[b] Department of Chemistry, M. R. Government Arts College, Mannargudi 614 001, Tamil Nadu, India

[c] Department of Chemistry, Government Arts College, C-Mutlur 608 102, Chidambaram, Tamil Nadu, India

[d] Saveetha School of Engineering, Saveetha Institute of Medical and Technical Sciences (SIMATS), Chennai 602 105, Tamil Nadu, India

[e] Department of Civil Engineering, Yeungnam University, Gyeongsan, 38541, Republic of Korea

[f] Department of Chemistry, Shree Raghavendra Arts and Science College, Keezhamoongiladi 608 102, Chidambaram, India

[g] Department of Chemistry, College of Science, Taif University, P.O. Box 11099, Taif 21944, Saudi Arabia

E-mail: drgtnarayanan@gmail.com, thirunarayanan.g.10313@annamalaiuniversity.ac.in

Received 19 June 2025; accepted (revised) 25 September 2025

Two anilide derivatives have been synthesized with more than 85% yield using $FeCl_3$-bentonite acidic catalyst-supported rearrangement of their oximes. These anilides have been investigated by their physico-chemical constants and spectroscopic data. The effect of various acidic catalysts and solvents on the rearrangement has been studied. The DFT analysis, molecular docking, ADMET properties, and antimicrobial activities of these anilides have been assessed with corresponding ligand protein interaction nature and microbes.

Keywords: Anilides, $FeCl_3$-Bentonite, IR and NMR spectra, DFT analysis, Molecular docking, ADMET properties, Antimicrobial activities

Anilides or phenylamides are a class of organic compounds that belong to substituted amide derivatives of anilines. They are derived by the acidic-catalyzed Beckmann rearrangement[1] of their oximes or Friedel-Crafts acylation[2] of anilines. Alternatively, the reaction of derivatives of carboxylic acids, such as acid chlorides, esters, and anhydrides, with amine or carboxylic acids directly reacts with amines with dehydrating agents, giving anilides[3]. This synthetic methodology was not efficient for the synthesis of anilides due to low atom economy and high percentage of by-product formation. Hence, an efficient and sustainable synthetic procedure is needed for the synthesis of anilides. From the twelve principles of green chemistry, good atom-economy, very low-cost, and cheap catalyst-supported synthetic methodology was developed for the synthesis of anilides[4]. Numerous organic substances, such as cyanides, carbonyl compounds, oximes, alcohol, or amines, were employed as starting reactants for the synthesis of anilides under metal catalyst support. From the chemical history, the Beckmann rearrangement is the best reaction for the synthesis of anilides from oxime. Beckmann rearrangement is employed for the synthesis of numerous organic substances, including caprolactams from nylon-6 (Ref. 5). Sadaphal *et al*., reported the acetophenone-based anilides from Beckmann rearrangement of oximes in the catalytic amount of silica-supported sulphamic acid[6]. The 2-alkylthio-4-cyanopyridine-based anilides were synthesized from their acid chlorides with aniline in the presence of sodium hydroxide[7]. Okumura *et al*., reported the synthesis of *N*-methyl-*N*-(3-methylphenyl) cyclohexane carboxamide anils by the $Ni(cod)_2$ catalyzed reaction of its carboxamide and alkene in toluene medium[8]. Sorbonilide derivatives were synthesized through the oxalyl chloride reaction of sorbic acid and aniline in dichloromethane medium were studied by Alvarenga and his co-workers[9]. The reaction of hexanoic

† These authors contributed equally to this work.

anhydride and anilines in the presence of HCl gave Hexanoic anilides[10]. Josef *et al*., reported a reaction of cyclohexanone with hydroxylamine in an acid medium to give the cyclic amide caprolactam[11]. Phipps *et al*., reported the arylation of anilides by copper (II) catalysts[12]. Nagaraju *et al*.[13] studied the influence of substituents at various positions of anilines for the synthesis of arylated anilides using copper acetate catalyst. Blagbrough *et al*.[14] reported the conversion of carboxylic acids into carboxylic amide (peptide) using isocyanates. Hussein *et al*.[15] prepared various aryl anilides such as morpholino-based anilides, Hantzsch amides[16], benzothiazine-based anilides[17] using sodium acetate and piperidine in ethanol as catalysts. Alkahtani *et al*.,[18] employed potassium carbonate supported stirring in a RT method for the synthesis of 90% yield of 2-[(4-oxo-3-(4-sulfamoylphenylethyl)-3,4-dihydroquinazolin-2-yl)thio]-*N*-substituted-amides from 4-(2-(4-oxo-2-thioxo-1,4-dihydroquinazolin-3(2*H*)-yl)ethyl) benzenesulfonamide and 2-chloro-*N*-substituted amide in acetone medium. Thionyl chloride supported [3, 3]-sigmatropic rearrangement of hydroxamic acid and hydroxylamine gave 2-chloroanilide and anilide derivatives were reported by Ayyangar *et al*.[19]. Zeolites beta containing Si/Al and MCM-41 catalyst[10, 12] supported the reaction of cyclododecanone oximes and acetophenone, giving acetanilides.

Beckmann rearrangement of ketoximes converted into anilides was reported by using highly effective high-yielding catalyst such as Indium trifluoromethanesulfonate[13]. Anilide possess numerous biological activities, such as anti-mycobacterial[20,21], antifungal[22], larvicidal[23], turbeculostatic[24], insecticidal[25], herbicidal[26], anti-convulsant, anaesthetic, anti-proliferative, antiplaque, antiplatelet-aggregation and antioxidant[27-31]. Bouchain *et al*. reported the synthesis of sulphonamide anilides as efficient Histone Deacetylase and antiproliferative agents[32]. Narasimhan *et al*.[33] reported the $SOCl_2$ catalyzed synthesis of substituted anilides and investigated the antimicrobial and QSAR models. Significant biological activity of organic compounds is necessary for drug development; however, this activity alone does not qualify the compounds as medicines. Some compounds are excluded because of their low toxicity and bioavailability. Discrete Fourier Transform or Density Functional Theory (DFT) is a quantum-mechanical technique employed to estimate the electronic structure of atoms, molecules, and materials such as molecules and solids based on the electron density rather than the wave function, which is computationally less demanding. Yan *et al*., investigated the DFT calculated infrared spectrum of some amides and they observed the aggregable vibrations compared to spectrophotometer recorded spectrum[34]. The synthesis, DFT analysis of some fatty amides was reported by Nesrain *et al*.[35]. Juping *et al*., studied the mechanistic route of conversion of amide to aldehyde by DFT study[36]. The molecular structure and relative stability of cis and trans isomers of anilide derivatives were investigated by quantum mechanical-DFT computational study was reported by Cagardova *et al*.[37] ADMET analysis is one of the most important steps for predicting the pharmacokinetic and toxicological profiles of highly active drug-like compounds such as imine[38], cyclopeptides[39], phytochemicals[40,] and imidazoles[41]. Literature review reveals that past and present, unavailability of description regarding formulation, molecular docking, ADMET properties, and evaluation of bio-potencies of 2-naphthanilide and 2-benzofuranilides. Hence, the authors wish to synthesize of above anilides by $FeCl_3$-Bentonite catalyzed Beckmann rearrangement of corresponding oximes to study the DFT analysis, molecular docking, ADMET properties, and antimicrobial activities.

Results and Discussion

Currently, authors have synthesized anilides employing various acidic catalysts, assisted Beckmann rearrangement of oximes under ultrasound irradiation conditions. Analytical quantities of oximes **1** and **2** were converted into their anilides by the action of 0.35 g of solid ferric chloride-bentonite catalyst in ether medium under sonication. Both oximes were completely converted into anilide with 86% yields. This rearrangement follows a well-known acidic-catalyzed mechanism. Primarily, hydrogenation of the OH group of oximes from the acidic site of $FeCl_3$-Bentonite catalyst to form $=N\text{-}O^{+}H_2$. The second step is the removal of water, and the aryl group migrates to the nitrogen atom, and then the nitrogen atom carries a positive charge. The third stage is neutralization of the positive charge of the N atom by one of the π-bond electrons transferred from -C≡N moiety, and the C atom gets an electron deficiency, leading to the formation of a positive charge. The fourth step is the hydration of the C^{+} atom, then the oxygen atom of the water molecule has

an electron deficiency, creating a positive charge. Further removal of a proton neutralizes the positive charge of the oxygen atom. It exhibits that the keto-imino equilibrium leads to the formation of anilide. The possible mechanistic pathway of anilide formation was depicted in Scheme 1.

The consequences of the catalyst on the yield of the oximes were studied by the addition of the catalyst on the rearrangement from 0.05 to 0.5 g by increments of 0.05 g. Each addition of catalyst increases the yield from 34 to 86%. The increment of yield with the catalyst was tabulated in Table 1. Product yield quantity was not increased after reaching 0.35g of catalyst. Hence, this rearrangement required 0.35 g of catalyst for complete conversion of oxime into anilide, and it is tabulated in Fig. 1.

Also, we studied the catalyst optimization on this rearrangement for the conversion of oximes into anilides with various acidic catalysts such as SiO_2-H_2SO_4, SiO_2-H_3PO_4, SiO_2-PTS, Fly-ash-H_2SO_4, Fly-ash:H_3PO_4, Fly-ash:PTS, Fly-ash: BiO_2-SO_4. Fly-ash: SnO_2-SO_4, Zeolite-β-MCM-41, and $FeCl_3$-Bentonite under the above-mentioned same conditions. Among these catalysts, the $FeCl_3$-Bentonite catalyst gave a higher yield than the other. The optimization of the catalyst on the yield of the anilides are presented in Table 2.

Influence of solvents

This rearrangement was examined with some solvents such as acetonitrile, chloroform, dichloroethane, diethyl ether, dioxane, ethanol, methanol, propanol, and tetrahydrofuran with above mentioned experimental setup. Among these solvents, the ether medium gave a higher yield than the remaining solvents. Dioxane and tetrahydrofuran solvent phases gave the lowest yields. The influence

Table 1 — Effect of catalyst on the yield of anilides

Catalyst (g)	Yield (%)	
	Anilide 1	Anilide 2
0.05	34	36
0.1	41	44
0.15	49	51
0.2	58	60
0.25	67	69
0.3	74	78
0.35	86	86
0.4	86	86
0.45	86	86
0.5	86	86

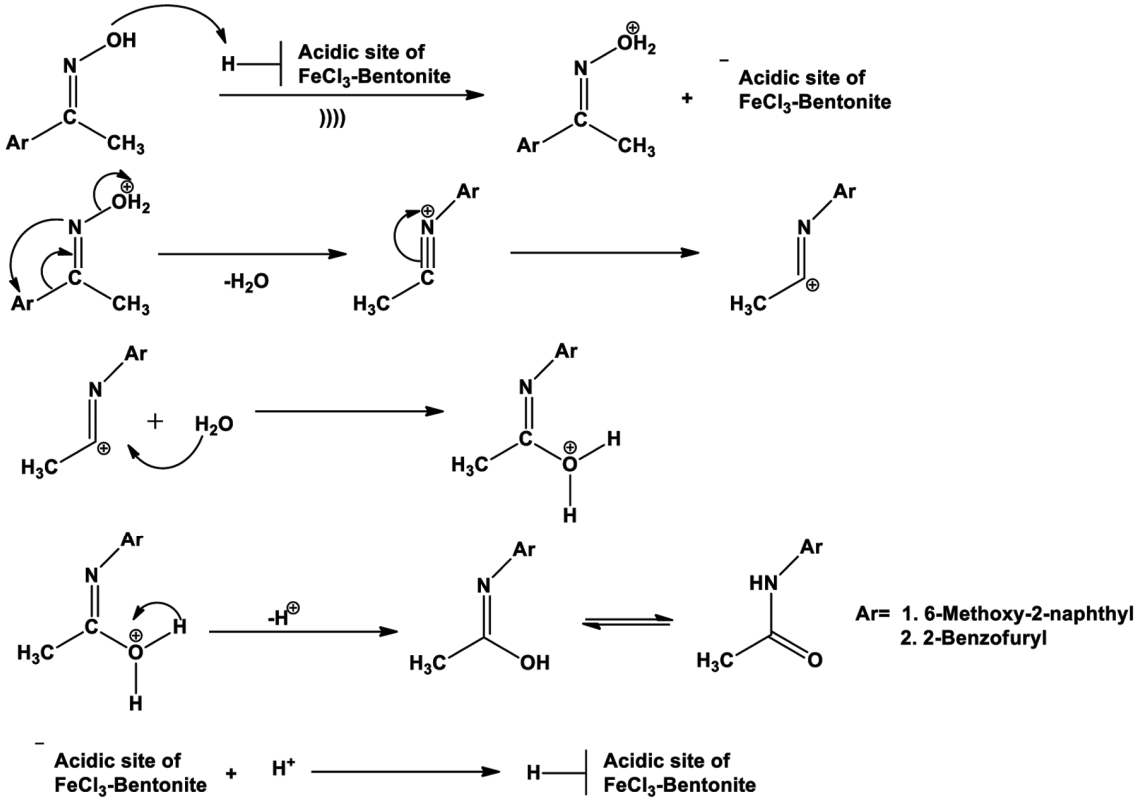

Scheme 1 — The proposed mechanistic pathway for the conversion of oxime into anilide by $FeCl_3$-Bentonite catalyst

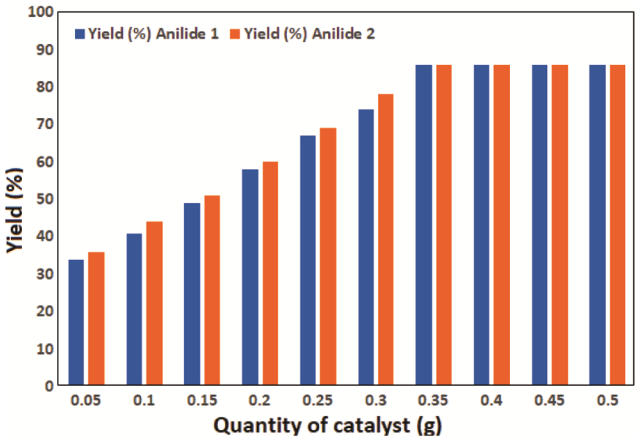

Fig. 1 — The illustration of the influence of the catalyst on the yield of anilides

Table 2 — Optimization of catalysts on the yield of anilides

Catalysts	Yield (%)	
	Anilide 1	Anilide 2
SiO_2-H_2SO_4	41	38
SiO_2-H_3PO_4	46	41
SiO_2-PTS	47	48
Fly-ash-H_2SO_4	49	52
Fly-ash:H_3PO_4	53	53
Fly-ash:PTS	55	54
Fly-ash: BiO_2-SO_4	50	43
Fly-ash: SnO_2-SO_4	48	57
Zeolite-β-MCM-41	63	62
$FeCl_3$-Bentonite	86	86

Table 3 — Influence of solvents on the yield of anilides

Solvent	Yield (%)	
	Anilide **1**	Anilide **2**
Acetonitrile	44	40
Chloroform	54	50
Dichloroethane	38	37
Diethyl ether	86	86
Dioxane	29	32
Ethanol	65	68
Methanol	66	68
Propanol	64	63
Tetrahydrofuran	33	35

of the solvents on the yield of anilides were presented in Table 3.

DFT- FMO, Electronic and Chemical Reactivity Studies

The optimized structure of anilides in Fig. 1, Fig. 2 and Fig. 3 was utilized for the calculation of global chemical reactivity parameters, frontier molecular orbital (HOMO and LUMO) analysis, and plotting the molecular electrostatic potentials. Frontier molecular

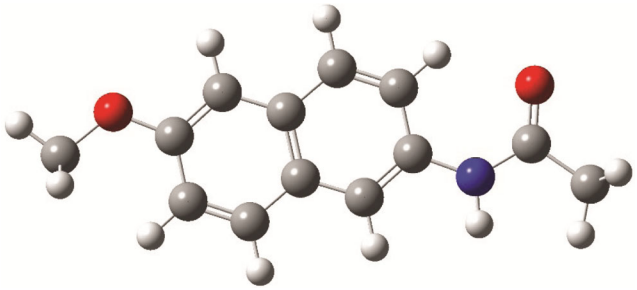

Fig. 2 — Optimized structure of N-(2-methoxynaphthalen-6-yl) acetamide (anilide **1**)

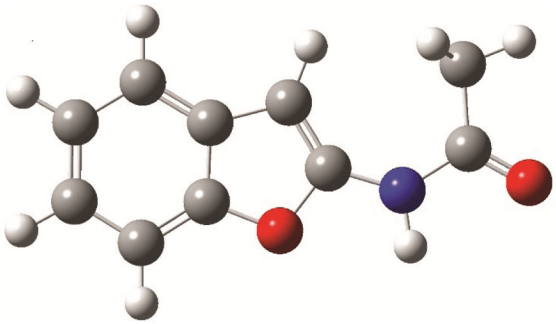

Fig. 3 — Optimized structure of N-(benzofuran-2-yl)acetamide (anilide **2**)

orbitals (FMOs) include the lowest occupied molecular orbital (LUMO) and the highest occupied molecular orbital (HOMO). HOMO-LUMO orbitals are the primary orbitals that contribute to a molecule's chemical stability. Whereas the LUMO denotes an electron acceptor and the HOMO denotes the capacity of donating electrons. The energy gap and HOMO-LUMO energies for title compounds have been computed in the current study utilizing the 6-311G (d, p) basis set at the B3LYP level. The frontier molecular orbital's (HOMO and LUMO) of synthesized compound are shown in Fig. 4.

Koopman's theorem served as the foundation for the parameters, Total energy (E), ionization potential (I), electron affinity (E), chemical hardness (η), electronic chemical potential (μ), chemical softness (σ), and global electrophilicity index (ω) are the chemical reactivity descriptors that were computed using DFT/B3LYP/6-311G (d, p) level. These values are shown in Table 4 which were computed using following equations (1-5).

$$\mu = -\tfrac{1}{2}(I + A) \quad \ldots (1)$$

$$\chi = 1/\mu \quad \ldots (2)$$

$$\eta = \tfrac{1}{2}(I - A) \quad \ldots (3)$$

$$\sigma = 1/\eta \quad \ldots (4)$$

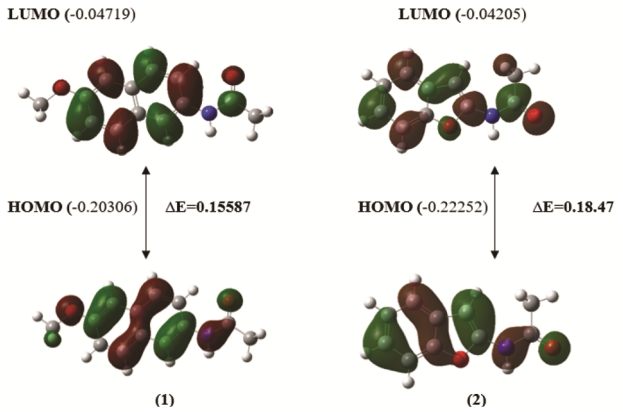

Fig. 4 — The HOMOs and LUMOs surfaces and energy values for anilides **1** and **2**

Table 4 — HOMO-LUMO energies of reactivity descriptors of anilides **1** and **2**

Parameters	Anilide 1	Anilide 2
E_{HOMO} (eV)	-0.20306	-0.22252
E_{LUMO} (eV)	-0.04719	-0.04205
ΔE (eV)	0.15587	0.18047
Electron affinity A	0.20306	0.22252
Ionization energy I	0.04719	0.04205
Chemical potential μ (eV)	-0.12512	-0.13228
Electronegativity χ (eV)	0.12512	0.13228
Chemical hardness η (eV)	0.07793	0.09023
Chemical softness σ $(eV)^{-1}$	12.8320	11.0821
Electrophilicity index ω (eV)	0.10045	0.09696

$$\omega = \mu^2/2\,\eta \quad \ldots (5)$$

These parameters are used to predict the stability and reactivity of a molecule. Chemical hardness (η), which is related to its stability, reactivity and donating electrons, it is a helpful concept for understanding how molecules behave. Hard molecules have large HOMO-LUMO gap hence, they resist change in electron distribution. Soft molecules with a small energy gap they easily gain or lose electrons. A molecule's softness (σ) is a characteristic that quantifies how reactive it is to chemicals. It is the value of hardness's reciprocal. Soft molecules have small excitation energies because of their lower HOMO-LUMO energy gap. As a result, electron density in a hard molecule, with a large gap, changes more hardly than a soft molecule. The anilide **1** has the lowest hardness value and highest chemical softness value compared with anilide **2.** Hence, anilide **1** has the most chemical and biological activities with drugs, but it is less stable. The global electrophilicity index (ω) measures the capacity of a species to accept electrons, it is utilized to explain the molecule's reactivity, toxicity, and dynamics. From the calculated values, anilide **1** (0.10045) is more toxic compared to anilide **2** (0.09696). The anilide **1** exhibits exceptional chemical strength and stability, according to the computed chemical potential and the electrophilicity index(ω).

MESP analysis

The molecular electrostatic potential surface study reveals the significant molecular characteristics like dipole moment, partial charges, chemical reactivity and also molecular size, shape and electrostatic potential regions with variation in the electron density distribution is shown by the existence of different unique colours. Blue and green shades denote zones with positive and zero electrostatic potentials, respectively, while red and yellow suggest zones with a high electron density. In anilide **1** the present study of the MESP plot indicates that the negative electrostatic potential (red in colour) is seen over the carbonyl group. So, the carbonyl group has more reactivity towards electrophile (H acceptor). The blue area, region of positive electrostatic potential, is situated above the hydrogen atoms. The anilide **1** and **2** electrostatic chemical potential is represented in Fig. 5 and Fig. 6.

Molecular docking study

The synthesized anilides **(1, 2)** as ligands were docked with Human lanosterol 14-α demethylase CYP51A1 protein inhibitor 3LD6 (Ref. 42-44) and revealed the binding energies of -7.11 and – 6.24 kcal/mol, respectively. The binding energy of anilide **1** is -7.11kcal/mol, and it exhibits one hydrogen bond interaction to the amino acid region HIS A:489 (histidine), three hydrophobic bond interactions such as ILE A:377, LEU A: 310, MET A:378 (Isoleucine, Leucine, and Methionine). The compound **2** shows binding energy of -6.24 kcal/mol and it displayed three hydrophobic bond interactions to amino acid region ALA A:444, PRO A:441 and VAL A:440 (Alanine, Proline and Valine), two electrostatic bond interactions such as ARG A:448 and LYS A:436 (Arginine and Lysine) and one hydrogen bond interaction to TYR A:439 (Tyrosine) amino acid residue. The binding energies, two- and three-dimensional docking poses of anilides **1** and **2** are shown in Table 5.

ADMET study: *In Silico*-Predicted Physicochemical and Pharmacokinetic Properties

Based on the information provided from ADMET analysis, the compound′s molecular weights are

less than 500 g/mol, and their rotational bond number and topological polar surface area (TPSA) are still below 140 Å² and 10, respectively. The ADME radar absorption structure of anilides was illustrated in Fig. 7. This implies that the produced substance may interact with targets in a variety of ways. These compounds may be soluble in aqueous solutions, as shown by their LogP values which are less than 5. Additionally, the donor and acceptor numbers for hydrogen bonds are less than 5 and 10, respectively. Consequently, the synthesized molecule exhibits exceptional oral bioavailability qualities and complies with the Lipinski, Veber′s, Egan, and Muegge requirements.

An important factor determining through numerous ADME properties is lipophilicity. The dispersion of drug molecules is measured by the Log P value between the lipid composition of the cell membrane and the aqueous environment outside of it. Accordingly, substances with a lower Log P value are more polar and have less permeability crosswise lipid bilayers. On the other hand, substances with a higher Log P value become less polar and less soluble in water. Aniline **1** shows a lower value of 1.69 than Anilide **2** shows 2.37. The Lipinski rule of five, which consists of multiple groups of guidelines and procedures, was computed with current anilide substances, is another remarkable trait.

The investigated physicochemical and pharmacokinetic properties of the anilides were summarized in Table 6 and Table 7. These tables explored that these anilides displayed higher gastrointestinal absorption and they denoted fast incorporation and preoccupation of synthesized anilides in the small intestine. Anilides **1** and **2** display blood-brain barrier penetration, another essential prediction for Alzheimer's disease treatment. These results imply that anilides **1** and **2** have the ability to enter the central nervous system (CNS), which would make them effective in treating illnesses like AD.

The central nervous system is protected against xenobiotics by the permeability glycoprotein (P-gp).

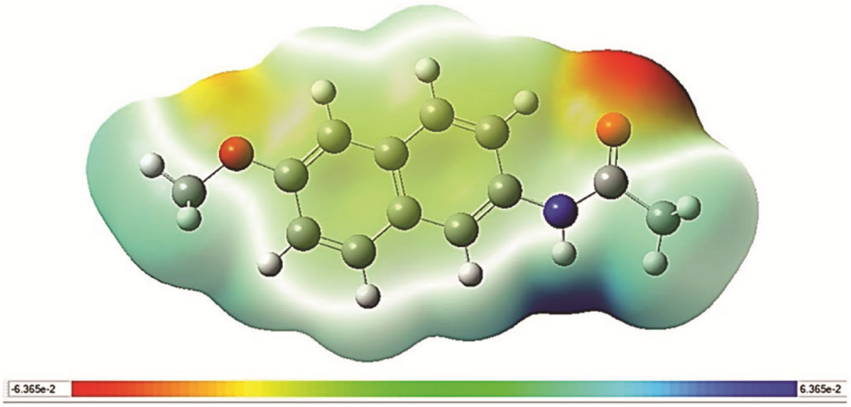

Fig. 5 — Molecular electrostatic potential for anilide **1**

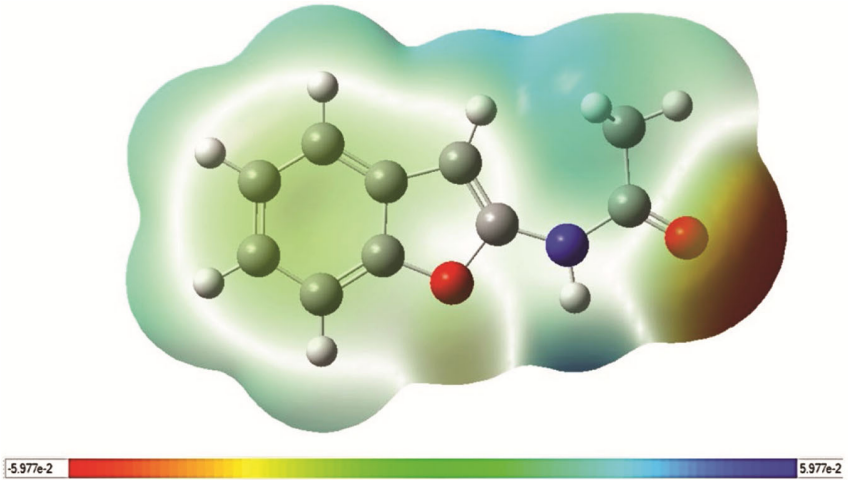

Fig. 6 — Molecular electrostatic potential for anilide **2**

Table 5- Binding energies and docking poses of synthesized anilides **1** and **2**.

Anilide	2D Image	3D Image	Binding energy (ΔG) kcal/mol
1	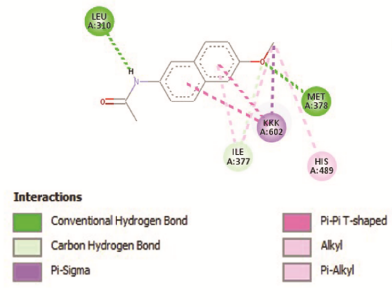	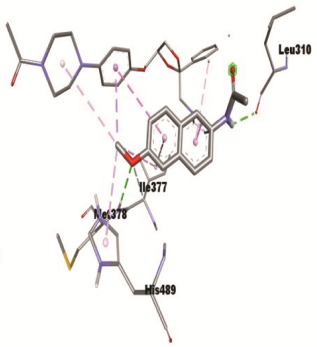	-7.11
2	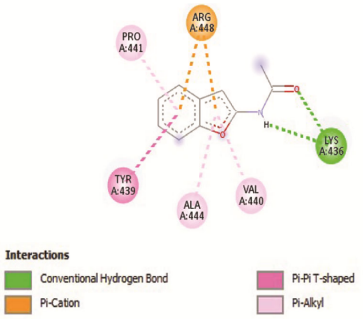	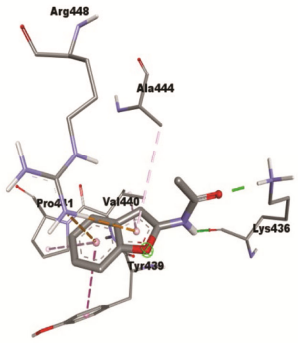	-6.24

Table 6 — ADME and physicochemical parameters of the anilide

Anilide	M. W.	HBD	HBA	NRB	TPSA	GI absorption	M Log P	BBB Permeability	Bio Availability	Lipinski Violation
1	215.25	1	2	3	38.33	High	2.37	Yes	0.55	0
2	175.18	1	2	2	42.24	High	1.69	Yes	0.55	0

Table 7 — Pharmacokinetic properties of synthesized anilides

Anilide	p-gp Substrate	Metabolic enzymes Inhibitors						Log Kp (cm/s)
		CYP1A2	CYP2C19	CYP2C9	CYP2D6	CYP2D6	CYP3A4	
1	No	Yes	No	No	No	No	No	-5.97
2	No	Yes	No	No	No	No	No	-5.91

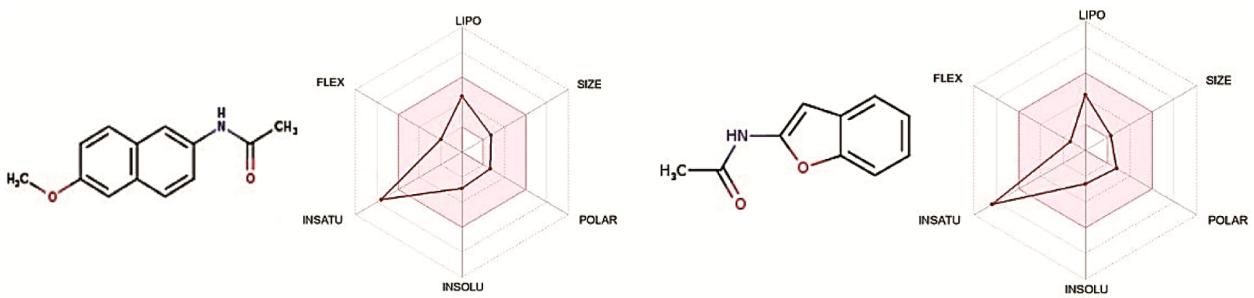

Fig. 7 — The ADME radar absorption structure of anilides

The synthesized compounds are efficient xenobiotic inhibitors and P-gp substrates, as shown in Table 7. Table 7 shows that while the metabolism of other metabolic enzymes is effective, that of CYP1A2 metabolic enzymes is inhibited. Compared to the expected water solubilities, in Table 8, anilides 1 and 2 are more soluble in the aqueous class, whereas in the SILICOS-IT class, anilide 1 is moderately soluble. The bioavailability of synthesized anilides is illustrated in Fig. 8. Furthermore, the two synthesized compounds estimated criterion $LogP_{0/w}$ (Lipophilicity) values of 1.81 and 2.37, suggesting that the anilides may possess responsible ADME properties in the lipid segments.

Antimicrobial activities

The assessed antibacterial and antifungal potencies by means of the mm of zone of inhibition[45-56] of synthesized anilides are summarized in Table 9. The numerical bar diagram of antibacterial potencies of anilides is depicted in Fig. 9. Anilide **1** possesses good antibacterial activity against all microbes. Anilide **2** exhibits good antibacterial actions against all microbes except *Streptococcus agalactiae.*

Both anilides show good antifungal activity against *Penicillium chrysogenum* and *Trichoderma viride*. The moderate activity was observed for this anilide against *Aspergillus niger* and *Candida albicans* fungal stains.

Table 9 — Antimicrobial potencies by means of mm of zone of inhibitions of synthesized anilides

Microbes	Anilide 1	Anilide 2
Antibacterial activity		
Streptococcus agalactiae	15	13
Enterococcus	16	16
Escherichia coli	16	18
Pseudomonas aeruginosa	14	17
Standard (Amoxicillin)	17	20
Antifungal activity		
Aspergillus niger	14	15
Candida albicans	13	10
Penicillium chrysogenum	18	16
Trichoderma viride	19	20
Standard (Miconazole)	21	21

Table 8 — Lipophilicity and water solubility properties of the synthesized anilides

Anilide	Log S (ESOL)			Log S(Ali)			Log S(SILICOS-IT)			Lipophilicity
	ESOL	Solubility mg/mL	Class	Ali	Solubility mg/mL	Class	Silicos-IT	Solubility mg/mL	Class	Consensus Log P
1	-2.90	2.7	Soluble	-2.76	3.7	Soluble	-4.59	5.47	Moderately Soluble	2.37
2	-2.60	4.36	Soluble	-2.58	4.65	Soluble	-3.67	3.74	Soluble	1.81

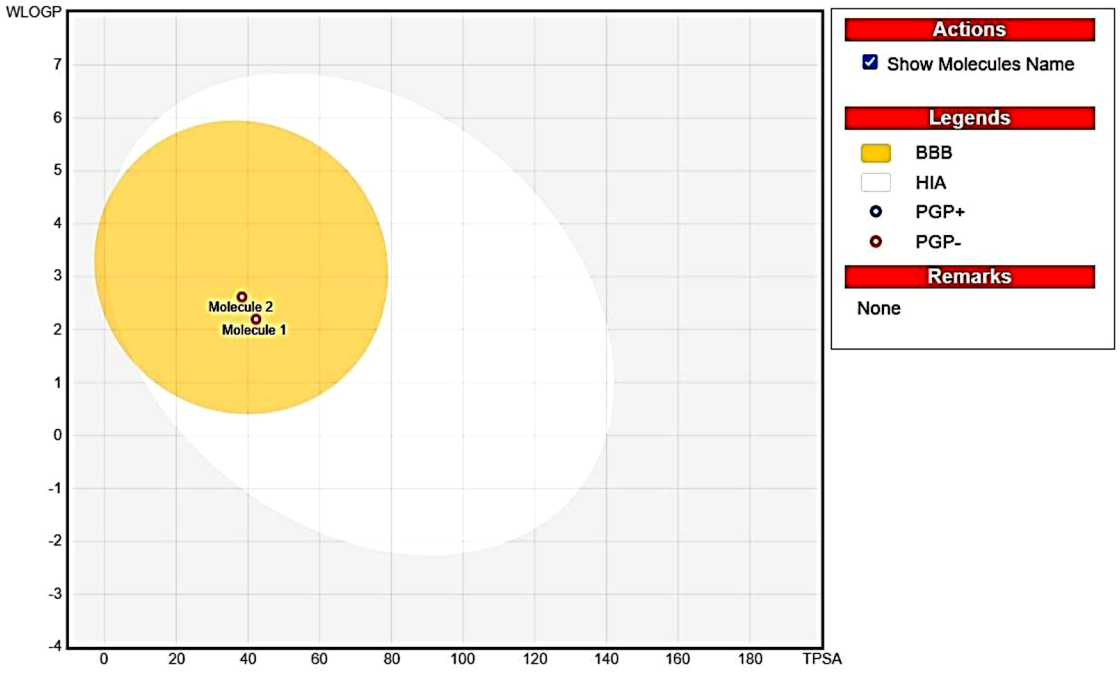

Fig. 8 — Boiled egg model for the bioavailability of anilides **1** and **2**

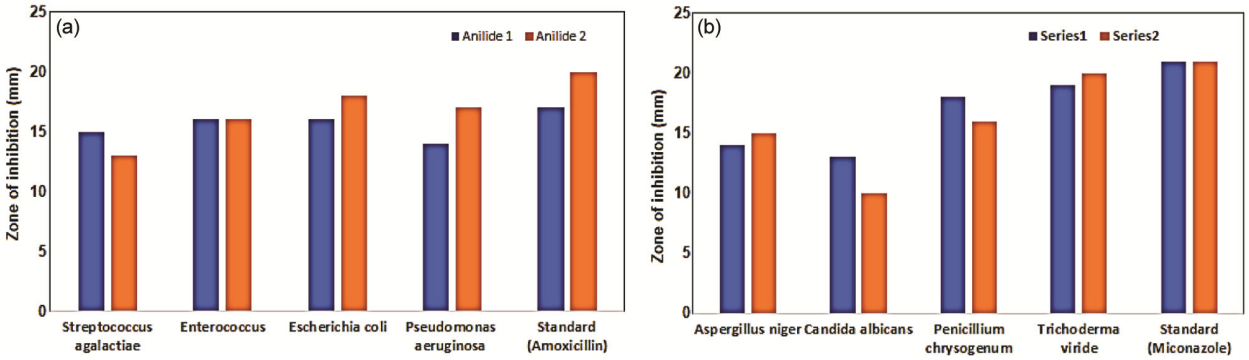

Fig. 9 — The clustered column chart representation of antimicrobial activities of synthesized anilides

Experimental Section

Materials and methods

In this current investigation, the Sigma-Aldrich chemical company's chemicals and solvents were employed. The melting points of synthesized anilides were determined in open glass capillaries by means of the Mettler FP51 melting point device. Infrared spectra of synthesized anilides have been recorded in an Avatar-300 Thermo Nicolet Fourier Transform Infrared Spectrophotometer using KBr discs with a frequency range of 4000-400 cm^{-1}. NMR spectra for all anilides were recorded in the Bruker AV 400 spectrometer operated at 400 MHz was used for ^{1}H NMR spectra and 100 MHz for ^{13}C NMR spectra in $CDCl_3$ solvent, utilizing TMS as an internal standard. Elemental analysis was performed with a Perkin-Elmer 240 CHN analyzer. Mass spectra of all compounds were recorded in the Varian-Saturn 2200 GC-MS spectrometer by means of the FAB technique in chemical ionization mode. The nutrient broth, Mueller-Hinton Agar, potato dextrose agar, tween-80 solution, and other necessary materials for microbial studies were obtained from Hi-Media, Mumbai.

General procedure for the synthesis of anilides

About 2 mmol of oximes[57], 0.35 g of $FeCl_3$-Bentonite[58] catalyst, and 20 mL of ether were taken in a 100 mL conical flask. The conical flask was equipped with a double surface condenser, and ice-cold water was circulated. The reactants were ultrasonicated for 18 minutes at 60 °C in an ultrasonicator containing water (CITIZEN ULTRASOUND SONICTOR, 5L, 120 W, HF 90 W, 40 kHz, 220-240V AC/50 Hz) (Scheme 2). The performance of the reaction was observed by TLC. After the complete conversion of oxime to anilides, distillation of the solvent afforded the product. The crude anilides were recrystallized using ethanol, gave glittering, curd white solids, and were dried in a desiccator.

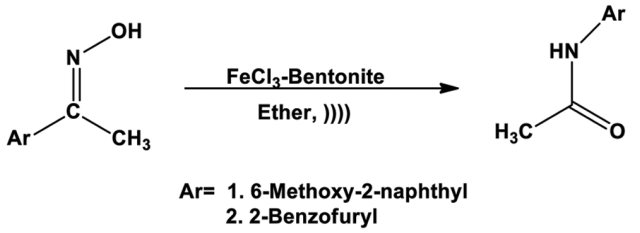

Scheme 2 — Synthesis of anilides by the acidic $FeCl_3$-bentonite catalyzed rearrangement of oximes under ultrasonication

Synthesized anilides were analyzed using their physico-chemical and spectroscopic data. These data strongly support the formation of anilides. The complete characterization of the anilides are as,

N-(6-Methoxynaphthalen-2-yl)acetamide (1): Curd white solid, Yield: 86%, m.p. 154 - 159°C. IR (KBr, ν, cm^{-1}): 3471, 2787,1654, 1432; ^{1}H NMR ($CDCl_3$, 400MHz, δ, ppm): 2.19 (s, 1H, CH_3), 3.99 (s, 1H, -OCH_3), 7.06 -8.04 (m, 6H, Ar-H), 8.24 (s, 1H, NH); ^{13}C NMR ($CDCl_3$, 100MHz, δ, ppm): 31.05 (-CH_3), 57.13 (-OCH_3), 157.27 (C-N),168.78 (C=O), 105.82 – 133.64 (Ar-C); MW: 215; MF: $C_{13}H_{13}NO_2$; Anal. Found (Calcd): C, 72.56 (72.54); H, 6.06(6.09); N, 6.49(6.51). Mass (m/z): 215, 200, 184, 172, 159, 157, 109, 106, 58, 56, 43, 31, 15.

N-(Benzofuran-2-yl)acetamide (2): Curd white solid, Yield: 81%, m.p. 172 - 173°C. IR (KBr, ν, cm^{-1}): 3335, 2917, 1640; ^{1}H NMR ($CDCl_3$, 400MHz, δ, ppm): 1.55 (s, 1H, CH_3), 7.26 -7.84 (m, 6H, Ar-H), 8.52 (s, 1H, NH); ^{13}C NMR ($CDCl_3$, 100MHz, δ, ppm): 29.70 (-CH_3), 176.32 (C=O), 112.32 – 134.74 (Ar. C); MW: 175; MF: $C_{10}H_9NO_2$; Anal. Found (Calcd.): C, 68.58(68.56); H, 5.16(5.18); N, 7.94(8.00). Mass (m/z): 175, 160, 149, 132, 117, 99, 76, 58, 43, 26, 15.

DFT-Computational Details

The synthesized compound was computed with DFT method using Gaussian-05(W) software. In order to examine the synthesized compound's theoretical parameters, DFT/B3LYP 6311 G (d, p) basis set, geometry was optimized.

Molecular docking analysis

The geometries of the prepared anilides were drawn from Chem Draw software. The geometries of anilides were optimized and transformed to a PDB setup using Open Babel software. A docking study was carried out for the allocated geometries of anilides. The 3D geometry of proteins was obtained from the Protein Data Bank (PDB) (www.rcsb.org): Human lanosterol 14-α demethylase CYP51A1 protein inhibitor (PDB: 3LD6)[42-44]. The steps followed for hostor construction. The initial step consists of the elimination of heteroatoms (water and ions), followed by adding a proton. The third step is charge computation. The dynamic regions were derived by applying lattice boxes of accurate dimensions around the bonded ligands. The docking investigations were explored using Auto Dock Vina software, and the 2D and 3D docking poses were observed using Discovery Studio for clear visualization.

Measurement of ADMET properties

The Swiss ADME online tool was used in this study to evaluate the ADMET drug-like quality properties of anilides[59,60].

Measurement of antimicrobial activity

Antimicrobial potencies of the prepared anilides were investigated employing the Bauer-Kirby disc-diffusion method[61]. Here, each two-gram positive and gram-negative bacterial stains such as *Streptococcus agalactiae, Enterococcus, Escherichia coli,* and *Pseudomonas aeruginosa* were applied to assess of antibacterial activity of anilides. Four antifungal microbes such as *Aspergillus niger, Candida albicans, Penicillium chrysogenum*, *Trichoderma viride* were applied for measurement of antifungal actions of anilides through mm of zone of inhibition[62,63].

Conclusions

Solid acidic $FeCl_3$-Bentonite catalyst was employed for the synthesis of two anilides, such as N-(6-methoxynaphthalen-2-yl)acetamide **(1)** and N-(benzofuran-2-yl)acetamide **(2)** through the rearrangement of oximes under sonication. These anilides were analyzed by their physico-chemical and spectroscopical data. These data strongly supported the synthesized anilides. The effect of the catalyst was studied in this rearrangement, and experimentally, 0.35 g of catalyst was needed for this reaction. Optimization of other acidic catalysts was studied for this rearrangement. From the experimental result $FeCl_3$-Bentonite catalyst gave a higher yield than other catalysts. The influence of solvent on the yield of anilides was studied. From this experiment, the ether medium gave a higher yield. Dioxane and tetrahydrofuran media gave lower yields. From DFT analysis anilide **1** exhibits exceptional chemical strength and stability. It is clear from the MESP that the carbonyl group is primarily covered by the negative electrostatic potential areas, indicating that this could be an attractive target for an electrophilic attack. Molecular docking study of these anilides shows the binding energies of –7.11 and –6.24 kcal/mol, respectively. Both anilides exhibit good antibacterial and antifungal activities against maximum microbes. According to the ADMET analysis results, both anilides can be utilized as clinical drugs for further development.

Acknowledgement

Authors thank the DST-NMR facility, Department of Chemistry, Annamalai University, Annamalaingar 608 002, India, for recording NMR spectra of anilides.

References

1 Kaur K & Srivastava S, *New J Chem*, 44 (2020) 18530.
2 Praveen Kumar Darsi S S, Nagamani K S, Rama Devi B, Naidu A & Dubey P K, *Der Pharm Chem*, 3 (2011) 35.
3 Montalbetti C A G N & Falque V, *Tetrahedron*, 61 (2005) 10827.
4 Lakshmireddy V M, Naga Veera Y, Reddy T J, Rao V J & China Raju B, *Asian J Org Chem*, 8 (2019) 1380.
5 Allen C L & Williams J M J, *Chem Soc Rev*, 40 (2011) 3405.
6 Sadhapal S, Markhele V, Soner S & Shingare M, *J Korean Chem Soc*, 52 (2008) 454.
7 Miletín M, Doležal M, Opletalová V, Hartl J, Král'ová K & Macháček M, *Molecules*, 6 (2001) 603.
8 Okumura S, Komine T, Shigeki E, Semba K & Nakao Y, *Angew Chem(Int. Edn.)*, 57 (2018) 929
9 Sartori *S K,* Alvarenga E S, Franco *C A,* Ramos D S & Oliveira D F, *Pest Man Sci*, 74 (2018) 1637.
10 Chen B, Hou X L, Li Y X & Wu Y D, *J Am Chem Soc*, 133 (2011) 7668.
11 Ritz J, Fuchs H, Kieczka H & Moran W C, *Caprolactam*, (John Wiley & Sons), 2000. (https://doi.org/10.1002/14356007.a05_031).
12 Phipps R J & Gaunt M J, *Science,* 3232 (2009) 1593.
13 Sharma A, Nagaraju K, Ananda Rao G, Gurubrahamam R & Chen K, *Asian J Org Chem*, 10 (2021)1567.

14 Blagbrough I S, Mackenzie N E, Ortiz C & Scott A I, *Tetrahedron Lett*, 27 (1986)1251.
15 Hussein A M, Gaby M S A, Shenab F A A, Rehim A M A, *Egypt J Chem*, 62 (2018) 1059.
16 Van Arman S A, Zimmet A J & Murray I E, *J Org Chem,* 81 (2016) 3528.
17 Ukrainets I V, Petrushova L A, Shishkina S V, Sidorenk L V, Sim G & Kryvanych O V, *Sci Pharm*, 84 (2016) 523.
18 Alkahtani H M, Abdalla A N, Obaidullah A J, Alanazi M M, Almehizia A A, Alanazi M G, Ahmed A Y, Alwassil O I, Darwish H W, Abdel-Aziz A A M & El-Azab A S, Bioorg Chem, 95 (2020) 103461.
19 Ayyangar N R, Naik S N & Srinivasan K V, *Tetrahedron Lett,* 31 (1990) 3217.
20 Doležal M, Vičík R, Miletín M & Král'ová K, *Chem Papers*, 54 (2000) 245.
21 Zitko J. Servusová B, Janoutová A, Paterová P, Mandíková J & Garaj V, *Bioorg Med Chem*, 23 (2015) 174.
22 Buchenaeur H, *Pest Sci*, 6 (1975) 525.
23 Nakagawa Y, Izumi K, Oikawa N, Kurozumi A, Iwamura H & Fujita T, *Pest Biochem Phy*, 4 (1991) 12.
24 Kayukova L A & Berikova E A, *Pharm Chem J*, 54 (2020) 555.
25 Tsikolia M, Bernier U R, Coy M R, Chalaire KC & Becnel J J, *Pest Biochem Phy*, 107 (2013) 138.
26 Doležal M, Hartl J, Miletín M, Macháček M & Král'ová K, *Chem Papers*, 53 (1999) 126.
27 Schultz H W, *J Pharm Sci*, 52 (2006) 503.
28 Niewiadomy A, Matisiak J & Macik-Niewiadomy G, *Euro J Pharm Sci*, 13 (2001) 243.
29 Ragavendran J V, Sriram D, Patel S K, Reddy I V, Bharathwazan N, Stables J & Yogeeswari P, *Euro J Med Chem*, 42 (2007) 146.
30 Biagi G, Giorgi I, Livi O, Nardi A, Calderone V, Martelli A, Martinotti E & LeRoy S O, *Euro J Med Chem*, 39 (2004) 491.
31 Aydin O N, Eyigor M & Aydin N, *Euro J Anaesthol*, 18 (2001) 687.
32 Bouchain G & Delorme D, *Curr Med Chem*, 10 (2003) 2359.
33 Narasimhan B, Narang R, Judge V, Ohlan R & Ohlan S, *Arkivoc*, 15 (2007) 112.
34 Yan J**,** Xiaoliang Y, Zhi J, Linhui Z, Nana M, Dejun C, Xianbin J, Junming T & Yilin C, *ACS Omega*, 5 (2020) 8572.
35 Nesrain F, Anis R A M, Shahla A, Norazilawati M S & Rosiyah Y, *Bioorg Chem*, 135 (2023) 106511.
36 Juping W, Huiying X, Hui G, Cheng-Yong S, Cunyuan Z & David L P, *Organomet*, 29 (2010) 42.
37 Cagardová D, Poliak P & Lukeš V, *Acta Chim Slova,* 10 (2017) 144-151.
38 Dinesh kumar N, Thirunarayanan G, Elancheran R, Suppuraj P, Guganathan L, Sivasakthikumar R, Ramkuma S & Swaminathan M, *J Mol Struct*, 1322 (2025) 140603.
39 Flores-Holguin N, Frau J & Glossman-Mitnik D, *Chem Open*, 10 (2021) 1142.
40 Bultum L E, Tolossa G B, Kim G, Known C & Lee D, *Sci Report*, 12 (2022) 22221. (https://doi.org/10.1038/s41598-022-26446-x).
41 Han H, Shaker B, Lee J H, Choi S, Yoon, S, Sing M, Basith S, Cui M, Ahn S, An J, Kang S, Yeom M S & Choi S, *J Chem Inf Model*, 65 (2025) 3215.
42 Murray G I, Patimalla S, Stewart K N, Miller I D & Heys S D, *Histopathol*, 57 (2010) 202.
43 Rooney P H, Telfer C, McFadyen M C E, Melvin W T & Murray G I, *Curr Cancer Drug Targets,* 4 (2004) 257.
44 Monostory K, Pascussi J M, Szabó P, Temesvári M, Köhalmy K, Acimovic J, Kocjan D, Kuzman D, Wilzewski B & Bernhardt R, *Drug Metabol Disposit,* 37 (2009) 375.
45 Dinesh Kumar S & Thirunarayanan G, *J Chil Chem Soc*, 61 (2019) 4265.
46 Ranganathan K, Kamalakkannan D, Suresh R, Sakthinathan S P, Arulkumaran R, Sundararajan R, Manikandan V & Thirunarayanan G, *Indian J Chem*, 58B (2019) 1131.
47 Suresh R, Sakthinathan S P, Kamalakkannan D, Muthuvel I & Thirunarayanan G, *Ovidius Univ Annal Chem*, 31 (2020) 55
48 Mala V, Muthuvel I, Thirunarayanan G, Sakthinathan S P, Arulkumaran R, Manikandan, V, Sundararajan R, Kamalakkannan D, Suresh R & Usha V, *Ovidius Univ Annal Chem*, 31 (2020) 152.
49 Manikandan V, Vanangamudi G, Arulkumarn R, Christhuraj P & Thirunarayanan G, *Indian J Chem*, 59B (2020) 399.
50 Dineshkumar S, Muthuvel I, Mayavel P, Markandan R, Usha V & Thirunarayanan G, *Indian J Chem*, 60B (2021) 1373.
51 Usha V, Thirunarayanan G & Manikandan S, *Indian J Chem*, 61 (2022) 521.
52 Muthuvel I, Manikandan S, Thirunarayanan G, Usha V & Sathiyendiran V, *Indian J Chem*, 62 (2023) 131.
53 Dinesh kumar N, Muthuvel I & Thirunarayanan G, *Indian J Chem,* 62 (2023) 906.
54 Boobalarasu V, Thirunarayanan G & Sivakumar K, *Curr Chem Lett*, 13 (2024)101.
55 Venkatraman R, Divya J, Gayathri P, Thirunarayanan G & Muthuvel I, *Ovidius Univ Annals Chem*, 35 (2024) 36.
56 Nalini S, Divya J, Gayathri P, Muthuvel I, Thirunarayanan G, Manikandan V & Usha V, *Indian J Chem*, 63 (2024) 557.
57 Gayathri P, Divya J, Muthuvel I, Mayavel P, Usha V, Nalini S, Manikandan V, Sundararajan R, Arulkumaran R, Sakthinathan S P & Thirunarayanan G, *Ovidius Univ Annal Chem,* 35 (2024) 146.
58 Muthuvel I, Dineshkumar S, Thirumurthy K, Krishnakumar B & Thirunarayanan G, *Indian J Chem*, 55B (2016) 252.
59 Diana A, Michielien O & Zoete V, *Sci Rep*, 7 (2017) 42717
60 Saghdani N, El-Abbouchi A, El-Brahmi N, Idir A, Rachedi K O, Berredjem M, Haloui R, Elkhattabi S Mouse H A, Hada T B & Bousmina M, *Comp Bio Chem* 113 (2024) 108214.
61 Bauer A W, Kirby W M M, Sherris J C & Truck M, *Am J Clin Pathol*, 45 (1966) 493.
62 P. Mayavel, J. Divya, P. Gayathri, S. Balasundari, V. Usha, I. Muthuvel, 4, Krishnakumar Balu, Shivakumara K N, Gurusamy Raman, G. Thirunarayanan, *Res Chem Intermed*, 50 (2024) 4503.
63 Dinesh Kumar N, Rajamohan K S, Selvakumar K, Rajamanickam D, Thirunarayanan G & Swaminathan M, *J Mol Struct*, 1339 (2025) 142824.